J. Biophotonics **6**, No. 11–12, 905–910 (2013) / **DOI** 10.1002/jbio.201200247

Journal of BIOPHOTONICS

LETTER

Localized micro-scale disruption of cells using laser-generated focused ultrasound

Hyoung Won Baac[**,1], *John Frampton*[2], *Jong G. Ok*[3], *Shuichi Takayama*[2], *and L. Jay Guo*[*,1,3]

[1] Department of Electrical Engineering and Computer Science, University of Michigan, Ann Arbor, MI 48109, USA
[2] Department of Biomedical Engineering, University of Michigan, Ann Arbor, MI 48109, USA
[3] Department of Mechanical Engineering, University of Michigan, Ann Arbor, MI 48109, USA

Received 28 December 2012, accepted 23 January 2013
Published online 19 February 2013

Key words: laser-generated focused ultrasound, cavitation, cell detachment, drug delivery

Supporting information for this article is available free of charge under http://dx.doi.org/10.1002/jbio.201200247

We utilize laser-generated focused ultrasound (LGFU) to create targeted mechanical disturbance on a few cells. The LGFU is transmitted through an optoacoustic lens that converts laser pulses into focused ultrasound. The tight focusing (<100 μm) and high peak pressure of the LGFU produces cavitational disturbances at a localized spot with micro-jetting and secondary shock-waves arising from micro-bubble collapse. We demonstrate that LGFU can be used as a non-contact, non-ionizing, high-precision tool to selectively detach a single cell from its culture substrate. Furthermore, we explore the possibility of biomolecule delivery in a small population of cells targeted by LGFU at pressure amplitudes below and above the cavitation threshold. We experimentally confirm that cavitational disruption is required for delivery of propidium iodide, a membrane-impermeable nucleic acid-binding dye, into cells.

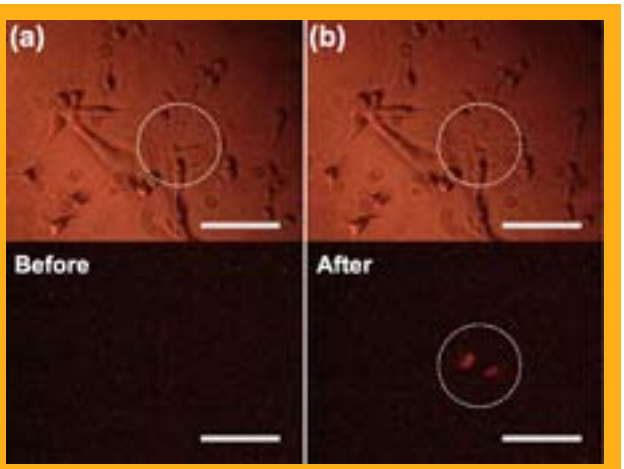

Biomolecule delivery by LGFU at the near-threshold regime for cavitation.

1. Introduction

Ultrasonic techniques can be used to modify or activate biochemical functions of cells and tissues in a non-invasive, localized, and temporally controlled manner [1–8]. At the cellular level, most of these techniques rely on acoustic cavitation to create liquid micro-jets, shear stress, and shock-waves that disrupt cell membranes [7–14]. This enhances uptake of membrane-impermeable molecules such as plasmid DNA and some drugs. These mechanical forces can also selectively remove cells from their culture substrates for cell harvesting and patterning [10–12].

* Corresponding author e-mail: guo@umich.edu.
** Current address: Harvard Medical School, Wellman Center for Photomedicine, Massachusetts General Hospital, 40 Blossom Street, Boston, MA 02114, USA.

For direct ultrasonic disruption, high-pressure amplitudes generated by focused transducers (e.g., shock-wave lithotripters and high-intensity focused ultrasound (HIFU) transducers) are required to produce shock effects and acoustic cavitation at a target location. However, the spatial accuracy of these conventional transducers approximates a focal zone of several millimeters or larger in diameter due to their low operation frequency (a few MHz) [9–14]. These transducers have been used to analyze macro-scale shear stress and cavitation-induced effects on large populations of cells [9, 10]; however, it is difficult to elucidate microscopic interactions between localized acoustic effects and individual cells.

Preformed micro-bubbles can be used to localize mechanical forces on cells. These bubble agents can be prepared with bio-functional units that target them to cells. The bubbles can then be collapsed under focused ultrasound with moderate pressure amplitudes (~1 MPa), leading to mechanical cell disruption that triggers various biochemical phenomena within the cells [15, 16]. Unfortunately, these techniques require additional methods for micro-bubble delivery that often involve preparation of microfluidic devices for *in vitro* studies [13, 14] or injection channels for *in vivo* delivery [5]. Moreover, the efficiency of micro-bubble disruption depends on micro-bubble location (*i.e.,* proximity to cells) [13]. Thus, it would be advantageous to develop more consistent and predictable approaches for targeting ultrasound to single cells.

Laser-generated focused ultrasound (LGFU) produces high-amplitude (>50 MPa), high-frequency (>15 MHz) acoustic pressure within a small focal spot (<100 μm diameter) [17]. LGFU uses an optoacoustic lens with a nano-composite light-absorbing layer [18] to convert a nano-second laser pulse into a focused acoustic pulse. Since this acoustic pulse has both high peak-positive and peak-negative amplitudes, it can generate shock effects as well as acoustic cavitation forming transient micro-bubbles. This technique has an order-of-magnitude higher accuracy than conventional high-pressure transducers. With such precise localization, it is essential to directly explore microscopic cell responses to high-frequency, high-amplitude acoustic pressure.

In this report, we used LGFU to generate micro-scale ultrasonic disruption, targeting a focal spot that can cover a single or a few cells. We demonstrate that LGFU-induced forces are strong enough to detach a single cultured cell from its substrate without affecting neighboring cells. We also investigate the possibility of using LGFU-targeted disruption for biomolecule delivery across cell membranes without causing detachment. We compare membrane responses to cavitational conditions by varying the LGFU amplitudes to achieve pressures below and above the cavitation threshold, demonstrating that acoustic cavitation is required for biomolecule entry into cells. We further discuss future applications of LGFU-induced membrane disruption.

2. Experimental

2.1 LGFU Setup

For optoacoustic generation of the high-frequency focused ultrasound, a 6-ns pulsed laser beam with 532-nm wavelength and 20-Hz repetition rate (Surelite I-20, Continuum, Santa Clara, CA) was used to irradiate a carbon nanotube (CNT)-coated optoacoustic lens (12 mm in diameter and 11.46 mm in radius-of-curvature). The 6-dB focal width of the LGFU was 100 μm as characterized using a fiber-optic hydrophone (bandwidth up to 75 MHz). The experimental setup for LGFU measurement was described in [17]. We confirmed transient micro-bubbles formed at glass substrates by time-domain signals at the detector and high-speed camera recordings.

For cell detachment and membrane disruption experiments, the LGFU setup was combined with an inverted microscope (supporting information S1). Briefly, the ultrasonic focal plane was aligned with cell culture substrate on the microscope stage. Halogen and mercury lamps were used to illuminate the sample for bright-field and fluorescence imaging, respectively. Since the CNT-coated optoacoustic lens blocked some of the halogen illumination, the incidence direction of the halogen lamp was slanted. For easy focal alignment, the optoacoustic lens was attached to a fixed-length spacer to position the cell culture substrate.

2.2 Cell culture

We used a 4-inch petri-dish as a chamber filled with culture media. HeLa cells were cultured on plasma treated glass coverslips (No 1.5). The cells were maintained at 37 °C in DMEM with 10% fetal bovine serum and 1% antibiotic solution, in a humidified atmosphere containing 5% CO_2. Before experiments, the cultures were grown to 50–70% confluence. They were then transferred to the LGFU setup for cell detachment. For biomolecule delivery experiment, the medium was replaced with fresh medium containing 10 mL propidium iodide (PI). Here, we chose PI as a model biomolecule which is membrane-impermeable nucleic-acid binding dye. Once PI enters cells, it binds DNA and RNA, dramatically enhancing its fluorescence. As

the LGFU is only a source of disturbance, the characteristic fluorescence from PI is used as an indicator of ultrasonic trans-membrane delivery.

3. Results

LGFU was generated through the optoacoustic lens, leading to shock-waves and acoustic cavitation at the focal spot. Figure 1(a) shows the focal waveforms from pulsed laser irradiation at two different energies (E): a sub-threshold regime for cavitation ($E = 0.6E_{th}$) and an over-threshold regime ($E = 1.2E_{th}$). Here, we set E_{th} as a threshold laser energy per pulse to generate acoustic cavitation (10–11 mJ/pulse). A generation rate of cavitation (η), which is defined as number of times cavitation occurred per number of incident LGFU pulses, is ~50% at this threshold. The laser energy was measured at the location of the optoacoustic lens with ±10% error. The inset in Figure 1(a) shows an enlarged view of the waveforms. The asymmetric waveform at $E = 0.6E_{th}$ is a typical shape of LGFU. A stiff shock-front occurs at the leading edges for both waveforms. This is due to nonlinear evolution of acoustic propagation [19]. For LGFU with a laser energy of $E = 1.2E_{th}$, however, this waveform is severely distorted in the negative phase because cavitation occurs directly on the detector surface. The detector range was limited to ±0.4 V-peak in this setup. In this example, the temporal trace of the over-threshold waveform revealed that the cavitational disturbance was prolonged by 1.7 μs (i.e., 7.75–9.45 μs) on the detector surface. This corresponded to the approximate lifetime of the bubble, which could be increased up to tens of μs using higher laser energies.

Acoustic cavitation was observed using a high-speed camera (Figure 1(b)). We used a 1-mm thick glass plate for cavitation, removing the fiber-optic hydrophone from the focal zone. This confirmed cavitation on planar substrates (as used with cells), excluding acoustic diffraction due to the finite dimensions of the fiber hydrophone (diameter = 125 μm). Figure 1(b) shows a side view of a micro-bubble at the glass/water boundary generated using $E = 1.4$–$1.5E_{th}$. The bubble in this increased laser energy has a longer lifetime of >10 μs. Such longer lifetime allowed the camera to have a sufficient exposure time to capture the micro-bubble image clearly. The same image is also shown in Figure 1(c) but with an enhanced contrast. Interestingly, micro-jetting is clearly observed at the top of the bubble and at the interface with the glass (black arrows). The liquid jet from the top creates a stream towards the center of the bubble. The side jets generate shear stress along the glass surface. Bubble collapse generates secondary shock waves in addition to these forces. These on-demand cavitational disturbances deliver strong mechanical forces on microscopic targets such as cells.

LGFU was next used to detach cells with single-cell resolution (Figure 2). Using LGFU with a laser energy of $E = 1.4$–$1.5E_{th}$, we could remove individual cells without affecting neighboring cells. In this condition, $\eta \sim 100\%$. Single cells could be detached using fewer than 20 pulses, each of which were given in a 50 ms interval (i.e., total exposure time <1 second). Clusters containing several cells could be also

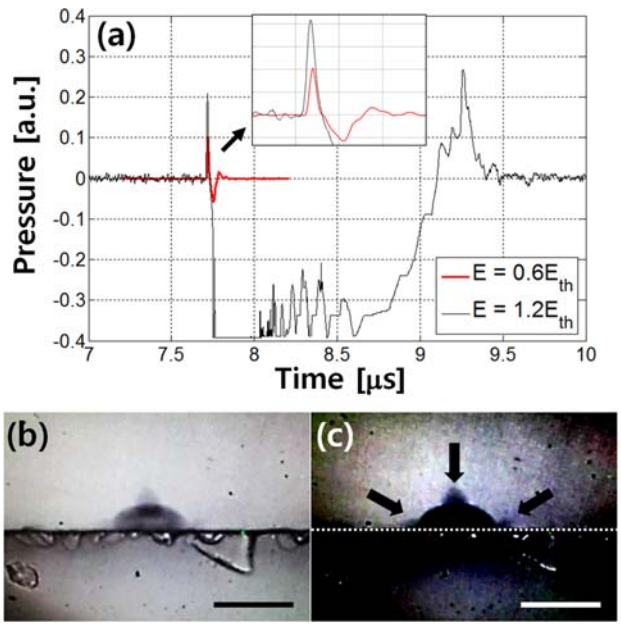

Figure 1 Cavitational disturbance formed on a glass substrate: (**a**) LGFU waveforms below and above the cavitation threshold. The inset compares two waveforms at the focal plane. A stiff shock-front is present in the positive phases for both waveforms. (**b**) Image of a transient micro-bubble (scale bar = 100 μm). The micro-bubble is shown under high brightness and low contrast. (**c**) The same image shown with enhanced contrast. Micro-jetting is indicated by black arrows. The white-dotted line indicates the glass/water boundary.

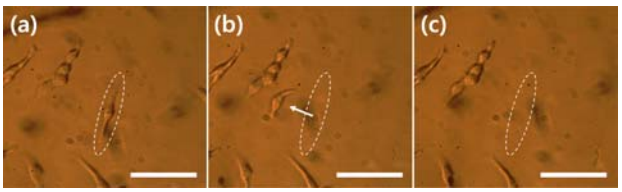

Figure 2 Cell detachment (scale bar = 100 μm). (**a**) The target cell is shown within the white-dotted region before LGFU. (**b**) An image taken immediately after cell detachment. The floating cell is shown, moving leftward. (**c**) The cell is completely removed, floating out of view.

removed using hundreds of pulses, depending on their shape and geometry. However, in the sub-threshold cavitation regime ($E < E_{th}$), cell detachment did not occur. This suggests that acoustic cavitation is required for cell detachment.

Then, we used our system for biomolecule delivery to cells. In order to avoid cell detachment, we reduced the laser energy to a near-threshold regime ($E = 0.9E_{th}$). Although this regime is below the nominal threshold E_{th}, we still have acoustic cavitation with a few % of generation rate. Moreover, the bubbles would have much shorter lifetimes (~1 μs) than those used for cell detachment (tens of μs). Therefore, LGFU at this near-threshold condition produces gentle, intermittent disturbances on cells.

Membrane disruption was confirmed using PI as a marker of trans-membrane delivery as mentioned above. The cells were placed in the PI-enriched medium. Figure 3(a) and (b) show bright-field and fluorescence images taken before LGFU. No fluorescence is observed in Figure 3(a), indicating that PI entry was blocked by the cell membrane. In Figure 3(b), the cells were exposed to LGFU (~200 pulses or 10-second exposure). The bottom image of Figure 3(b) clearly shows PI fluorescence in the targeted cells. Figure 3(c) shows the merged image of both bright-field and fluorescence of Figure 3(b), showing that cell morphology barely changed at the disrupted region. This suggests that LGFU can be used for precise disruption of cells (~60 μm diameter) without cell removal.

We further investigated cavitational dependence of membrane disruption, comparing two different regimes: sub-threshold and over-threshold to induce cavitation. Figure 3(d) and (e) show cell images before and after LGFU exposure at the sub-threshold

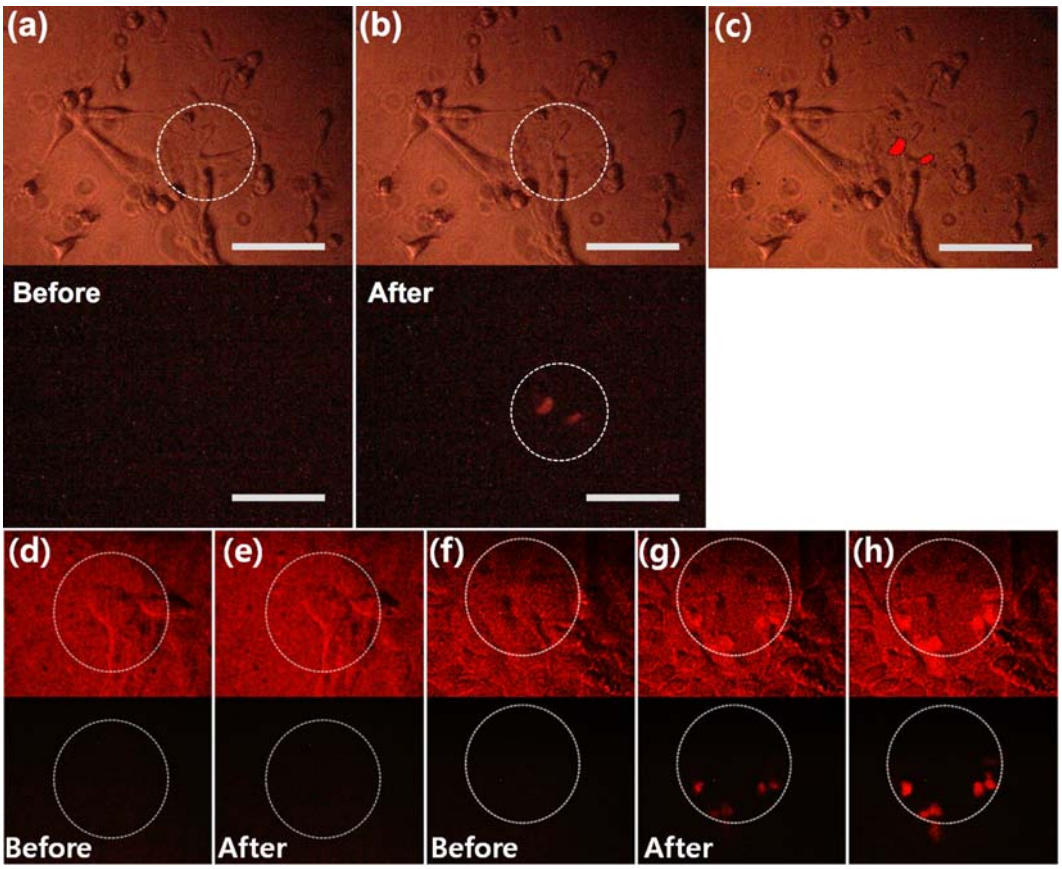

Figure 3. Biomolecule delivery by LGFU at the near-threshold regime for cavitation ($E = 0.9E_{th}$, 200 pulses) in (**a**)–(**c**), the sub-threshold ($E = 0.7$–$0.8E_{th}$, 12 000 pulses) in (**d**)–(**e**), and the over-threshold ($E = 1.2E_{th}$, 1200 pulses) in (**f**)–(**h**) (bright-field images in the above row and fluorescence in the bottom). White circles indicate the regions treated by LGFU (diameter = 100 μm, scale bar = 100 μm). (**a**) and (**b**) show cells before and after LGFU at the near-threshold. Two images of (**b**) are merged in (**c**). PI entry is observed but without cell morphology change. A new spot is chosen in (**d**). No fluorescence change is observed in (**e**) after LGFU exposure at the sub-threshold regime. Finally, another spot is chosen in (**f**). With LGFU above the cavitation threshold in (**g**), some cells are detached at the center, but PI entry is still observed in the periphery. After obtaining the images shown in (**g**), we turned off the LGFU and waited 2 min to obtain post-treatment images shown in (**h**).

condition ($E = 0.7–0.8E_{th}$). We could not observe any change in the PI fluorescence even after 10-min exposure (= 12 000 pulses), as shown in the bottom row of Figure 3(e). These results indicate that membrane disruption requires cavitational disturbance. Figure 3(f) and (g) show cells at another location before and after the LGFU exposure with $E = 1.2E_{th}$ (1200 pulses for 1 min). Although we observed some cell detachment at the center of the focal spot, the cells in the peripheral focal region remained intact for biomolecule delivery, resulting in PI labeling as shown in the bottom row of Figure 3(g). Figure 3(h) shows the same region 2 min after LGFU exposure. Brighter fluorescence in Figure 3(h) indicates that PI continued to enter the cells, diffusing within the cell and binding to nucleic acids in the cell nucleus. The disruption zone in Figure 3(g) was 100 μm, which is wider than the near-threshold condition (60 μm) in Figure 3(b).

4. Discussion

Using LGFU, we produced acoustic cavitation at targeted positions of <100 μm in diameter. Such tight focal spots require high-frequency ultrasound ($f > 15$ MHz) and therefore stronger tensile pressure (P) to induce cavitation, than those at the low-frequency regime ($P \propto f^{1/2}$) [20]. However, in our configuration, the pressure requirement is significantly relieved due to the existence of solid substrate. As LGFU is strongly reflected from the glass substrate, the tensile pressure is substantially increased within a shallow depth from the glass/water interface (<100 μm). Moreover, it plays a role as a supporting boundary for tiny seed bubbles before they grow and merge into a large bubble. Therefore, the cavitation threshold pressure is greatly reduced on the glass substrate as compared to cases without supporting boundaries [21]. We also confirmed that the cavitation can be formed on soft substrates such as tissues and elastomeric polymers but with higher LGFU amplitudes. The cavitation threshold can be further reduced using topographic structures [22]. The topographic approach would have an additional advantage in terms of regulating micro-scale shear forces in a designed manner.

In our system, the cavitational disturbance was controlled by the incident laser energy E which dictated the LGFU amplitude. In the over-threshold regime, $E > E_{th}$, the disruption was strong enough to cause cell detachment. By decreasing the LGFU to the near-threshold level, we could generate intermittent cavitation with a shorter lifetime. This moderate cavitation condition was successfully used to disrupt cell membranes without causing cell detachment or other morphological changes. However, future studies should access cell viability under various LGFU amplitudes and exposure times. In addition, the distance between the cavitation bubble and the cells should be considered as a significant variable.

We demonstrated biomolecule delivery using PI as a model cell-impermeable material. The LGFU technique might also be promising for delivery of other agents, such as nano-particles, which can be useful for controlled drug release. Conventionally, pulsed HIFU systems have been used already with some success to enhance localized nano-particle delivery into tissues [23, 24]. For the biomolecule delivery, the pulsed approach is preferred to avoid irreversible thermal deformation of cells and tissues. A thermal relaxation time in tissues is estimated as 6 ms over 100 μm diameter [25]. As our LGFU provides each pulse in 50 ms interval, heat deposition would be negligible despite the tight focal dimension.

5. Conclusion

LGFU produced cavitational disruptions at a micro-scale regime (<100 μm). Localized micro-jets surrounded the cavitation micro-bubbles, producing mechanical forces in addition to collapse-induced shock waves. We used these localized forces to detach single cells. We also applied our system for cell-impermeable biomolecule delivery. Membrane opening was confirmed by intra-cellular PI signal, depending on cavitational conditions. We could observe the targeted molecular delivery in high precision just over a few cells. We expect that our LGFU technique will be useful for high-precision cell detachment for harvesting and patterning as well as on-demand delivery of various molecular agents across biological membranes.

Acknowledgements The work is supported by the National Science Foundation and the National Institutes of Health, and a generous gift from the Beyster Foundation. The authors wish to acknowledge Prof. Zhen Xu of University of Michigan for using the high-speed camera and the fiber optic hydrophone.

References

[1] G. T. Haar, Prog. Biophys. Mole. Biol. **93**, 111–129 (2007).
[2] C. C. Coussios and R. A. Roy, Annu. Rev. Fluid Mech. **40**, 395–420 (2008).
[3] M. R. Prausnitz and R. Langer, Nat. Biotech. **26**(11), 1261–1268 (2008).
[4] B. E. Polat, D. Hart, R. Langer, and D. Blankschtein, J. Control. Release **152**, 330–348 (2011).

[5] J. J. Choi, M. Pernot, S. A. Small, and E. E. Konofagou, Ultrasound Med. Bio. **33**(1), 95–104 (2007).
[6] J. J. Choi, K. Selert, F. Vlachos, A. Wong, and E. E. Konofagou, Proc. Natl. Acad. Sci. USA **108**(40), 16539–16544 (2011).
[7] C. X. Deng, F. Sieling, H. Pan, and J. Cui, Ultrasound Med. Biol. **30**, 519–526 (2004).
[8] Y. Zhou, K. Yang, J. Cui, J. Y. Ye, and C. X. Deng, J. Control. Release **157**, 103–111 (2012).
[9] C.-D. Ohl, M. Arora, R. Ikink, N. de Jong, M. Versluis, M. Delius, and D. Lohse, Biophys. J. **91**, 4285–4295 (2006).
[10] C.-D. Ohl and B. Wolfrum, Biochim. Biophys. Acta **1624**, 131–138 (2003).
[11] L. Junge, C. D. Ohl, B. Wolfrum, M. Arora, and R. Ikink, Ultrasound Med. Biol. **29**(12), 1769–1776 (2003).
[12] R. Dijkink, S. Le Gac, E. Nijhuis, A. van den Berg, I. Vermes, A. Poot and C.-D. Ohl, Phys. Med. Biol. **53**, 375–390 (2008).
[13] K. Okada, N. Kudo, T. Kondo, and K. Yamamoto, J. Med. Ultrasonics **35**, 169–176 (2008).
[14] N. Kudo, K. Okada, and K. Yamamoto, Biophys. J. **96**, 4866–4876 (2009).
[15] G. A. Husseini and W. G. Pitt, Adv. Drug Deliv. Rev. **60**(10), 1137–1152 (2008).
[16] R. Suzuki, Y. Oda, N. Utoguchi, and K. Maruyama, J. Control. Release **149**, 36–41 (2011).
[17] H. W. Baac, J. G. Ok, A. Maxwell, K.-T. Lee, Y.-C. Chen, A. J. Hart, Z. Xu, E. Yoon, and L. J. Guo, Sci. Rep. **2**, 989 (2012).
[18] H. W. Baac, J. G. Ok, H. J. Park, T. Ling, S.-L. Chen, A. J. Hart, and L. J. Guo, Appl. Phys. Lett. **97**, 234104 (2010).
[19] M. F. Hamilton and D. T. Blackstock, Nonlinear Acoustics (Acoustical Society of America, Melville, 2008).
[20] R. E. Apfel and C. K. Holland, Ultrasound Med. Biol. **17**(2), 179–185 (1991).
[21] D. G. Shchukin, E. Skorb, V. Belova, and H. Möhwald, Adv. Mater. **23**(17), 1922–1934 (2011).
[22] E. Zwaan, S. Le Gac, K. Tsuji, and C.-D. Ohl, Phys. Rev. Lett. **98**, 254501 (2007).
[23] H. A. Hancock, L. H. Smith, J. Cuesta, A. K. Durrani, M. Angstadt, M. L. Palmeri, E. Kimmel, and V. Frenkel, Ultrasound Med. Biol. **35**(10), 1722–1736 (2009).
[24] B. E. O'Neill, H. Vo, M. Angstadt, K. P. C. Li, T. Quinn, and V. Frenkel, Ultrasound Med. Biol. **35**(3), 416–424 (2009).
[25] A. L. McKenzie, Phys. Med. Biol. **35**(9), 1175–1209 (1990).

